



**Journal Name**

COMMUNICATION

## Electronic Supporting Information (ESI)

### **An electrically controllable all-solid-state Au@graphene oxide actuator**

Qiuwei Shi,<sup>a</sup> Chengyi Hou,<sup>a</sup> Hongzhi Wang,<sup>\*a</sup> Qinghong Zhang,<sup>b</sup> and Yaogang Li<sup>\*b</sup>

<sup>a</sup> State Key Laboratory for Modification of Chemical Fibers and Polymer Materials, College of Materials Science and Engineering, Donghua University, Shanghai 201620, P. R. China. E-mail: wanghz@dhu.edu.cn; Fax: +86-021-67792855; Tel: +86-021-67792881.

<sup>b</sup> Engineering Research Center of Advanced Glasses Manufacturing Technology, Ministry of Education, College of Materials Science and Engineering, Donghua University, Shanghai 201620, P. R. China. E-mail: yaogang\_li@dhu.edu.cn; Fax: +86-021-67792855; Tel: +86-021-67792526.

#### **1. Experimental section**

##### **1.1 Materials**

Graphite powder (500 meshes, purity: 99%) was purchased from Shanghai Yifan Graphite Co., Ltd (China). Potassium permanganate, sulfuric acid, hydrogen peroxide (30 vol%) and hydrochloric acid were purchased from Sinopharm Chemical Reagent Co. Ltd (China). Gold wire (diameter: 1.0 mm, purity: 99.99%) was purchased from Beijing Zhongnuo New Materials Technology Co., Ltd (China). Silver wire (diameter: 0.05 mm, purity: 99.99%) was purchased from Alfa Aesar Chemicals Co.,

Ltd (China). Solar carer was purchased from the Uninwell International Co. Ltd. All reagents were analytical grade and used without further treatment.

### 1.2 Synthesis of GO

Graphite oxide was prepared by oxidation of flake graphite according to the modified Hummers' method.<sup>1,2</sup> Flake graphite powder (1 g) was added to concentrated sulfuric acid (23 mL, 0 °C) under stirring in an ice bath. Then, potassium permanganate (3 g) was added gradually with stirring. Successively, the mixture was stirred at 35 °C for 2 h. Then, distilled water (46 mL) was slowly added to the mixture with the temperature rise from 35 °C to 98 °C, and the mixture was maintained at 98 °C for 15 minutes. After that, the mixture was added to the preheated hydrogen peroxide solution (30%, 140 mL). Finally, the mixture was filtered and washed with hydrochloric acid aqueous solution (10 vol%, 250 mL) to remove metal ions. The yellow brown powder of GO is obtained after dried and grinded.

### 1.3 Synthesis of Au@GO bilayer film

Graphene oxide film (GOF) was first prepared by thermal evaporation of GO aqueous solution in drying oven. In a typical procedure, GO aqueous solution (5 mg mL<sup>-1</sup>, 60 mL) was poured into a cleanly polytetrafluoroethylene (PTFE) petri dish (internal diameter: 150 mm). Then the PTFE petri dish was moved in drying oven at 60 °C for 10 h to evaporate the water. After cooling to room temperature, the freestanding GOF was automatically separated from PTFE petri dish. Successively, the freestanding and flexible GOF was transferred into high vacuum resistance evaporation coating machine for gold-plating. Finally, the gold coated GO bilayer film (labeled as Au@GOF) was fabricated with a thermal evaporation coating system that the

evaporation was performed under high vacuum ( $3 \times 10^{-3}$  mbar at the beginning) and at the fast deposition mode ( $0.4 \text{ nm s}^{-1}$ ).

#### 1.4 Characterization and Measurements

The morphologies of the as-prepared samples were characterized using a high-resolution field emission scanning electron microscopy (FESEM, JSM-6700F) at 10.0 kV, and the photographs and videos were taken with a charge coupled device (CCD) video camera PowerShot G10, Canon. Fourier transform infrared (FTIR) spectra were recorded on a Nicolet NEXUS-670 spectrometer with KBr pellets. Raman spectra were carried out on a Renishaw in plus laser Raman spectrometer with  $\lambda_{\text{exc}} = 532 \text{ nm}$ . The X-ray diffraction (XRD) spectroscopy was performed on a Rigaku D/MAX 2550 V X-ray diffractometer with Cu K $\alpha$  irradiation ( $\lambda = 1.5406 \text{ \AA}$ ) with a step size of  $0.01^\circ$ . The operating voltage and current was 40 kV and 300 mA. The infrared thermal images and time versus temperature profiles were characterized by a FLIR Automation & Science Cameras A300 infrared thermometer. X-ray photoelectron spectroscopy (XPS) measurements were characterized with an SECA Lab 220i-XL spectrometer by using an unmonochromated Al K $\alpha$  (1486.6 eV) X-ray source and the typical detection depth is about 5 nm. Energy dispersive spectrometer (EDS) mapping of each element was taken with a JSM-6700F FESEM equipped with an Oxford Instruments EDS detector. AFM images were taken out using a Nanoscope IV SPM (Digital Instruments). The specific surface area of the GO film and Au@GO bilayer film was tested using physical adsorption of N<sub>2</sub> at liquid-nitrogen temperature on an automatic volumetric sorption analyzer ASAP 2020 (Quantachrome Instruments, USA). Mechanical property experiments of as-prepared products were conducted with a digital micrometer and an Instron universal material testing system (INSTRON

5969). The electro-mechanical characteristics was conducted with an electro-chemical station (CHI 760D, Shanghai Chenhua Instruments).

## 2. Supporting Figures

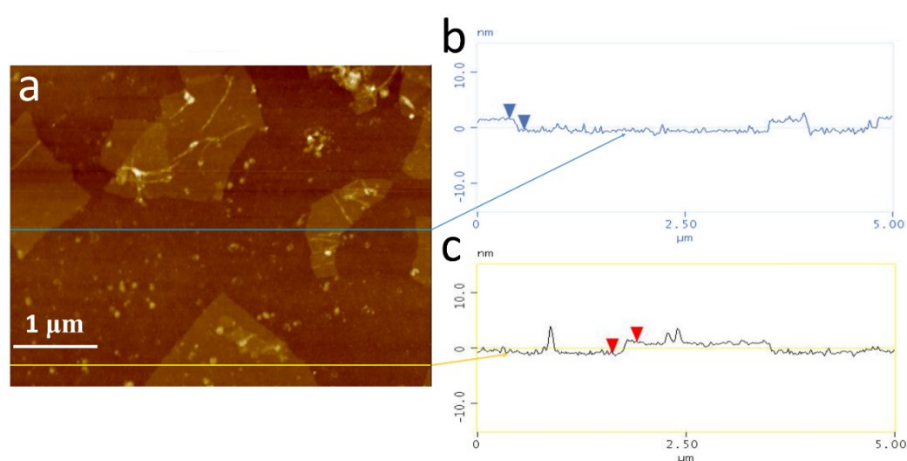


**Figure S1.** (a) AFM image of as prepared GO sheets; (b and c) height profile of the blue and yellow line in AFM image.

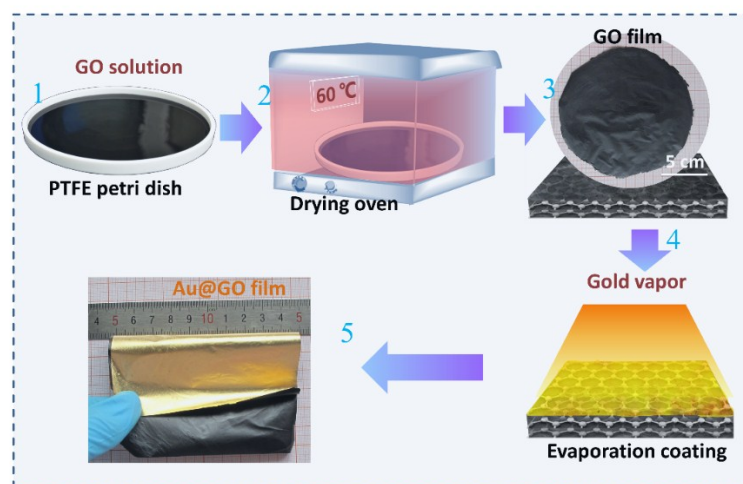


**Figure S2.** Schematic illustration of the thermal evaporation and evaporation coating process to fabricate the Au@GO bilayer film. Inset photograph show the actual morphology in the process.

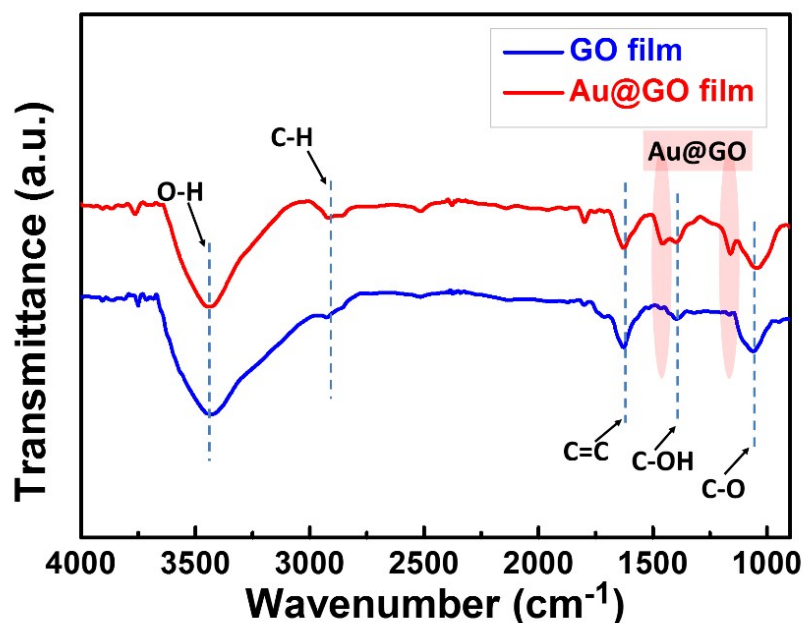


**Figure S3.** FTIR spectra of GO film and Au@GO film. Different spectroscopy measurements were taken to characterise the formation of Au@GO film. The FTIR spectra of the reference GO film indicates characteristic functional groups in the structure,<sup>3, 4</sup> including the O-H (3440 cm<sup>-1</sup>), C-H (2918 cm<sup>-1</sup>), *sp*<sup>2</sup>-hybridized C=C (1627 cm<sup>-1</sup>), C-OH (1398 cm<sup>-1</sup>) and C-O (1045 cm<sup>-1</sup>), as shown in Figure S4. The Au@GO film shows nearly similar FTIR spectra compared to the GO film, except for the new peaks at 1456 cm<sup>-1</sup> and 1159 cm<sup>-1</sup>, corresponding to the COOH and C-OH groups.<sup>5</sup> These results reveal that the Au has been covalently bonded to the COOH and C-OH groups of the GO sheet, according to the previous work.<sup>4, 5</sup>

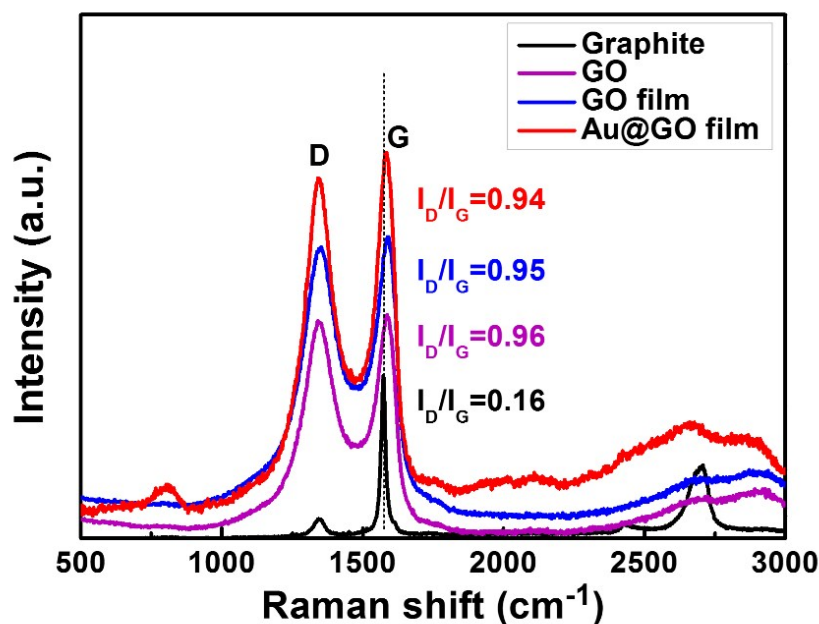


**Figure S4.** Raman spectrums of the graphite, GO, GO film and Au@GO film. The Raman spectra of initial precursor, intermediate and final products consists of distinct D and G band (Figure 1g),<sup>6, 7</sup> which are the breathing modes of six-atom rings and the high-frequency  $E_{2g}$  phonon at Brillouin zone centre.<sup>8</sup> Two general observations can easily be made from Figure 1g: (1) the intensity ratio of the D and G bands ( $I_D/I_G$ ) of graphite, GO, GO film Au@GO film are 0.16, 0.96, 0.95 and 0.94, respectively, (2) the G-band frequency of GO, GO film and Au@GO film were downshifted comparing to G-band frequency of graphite. This indicates that the process of preparation of GO introduce defects on graphene layers, but the thermal evaporation and evaporation coating procedure.

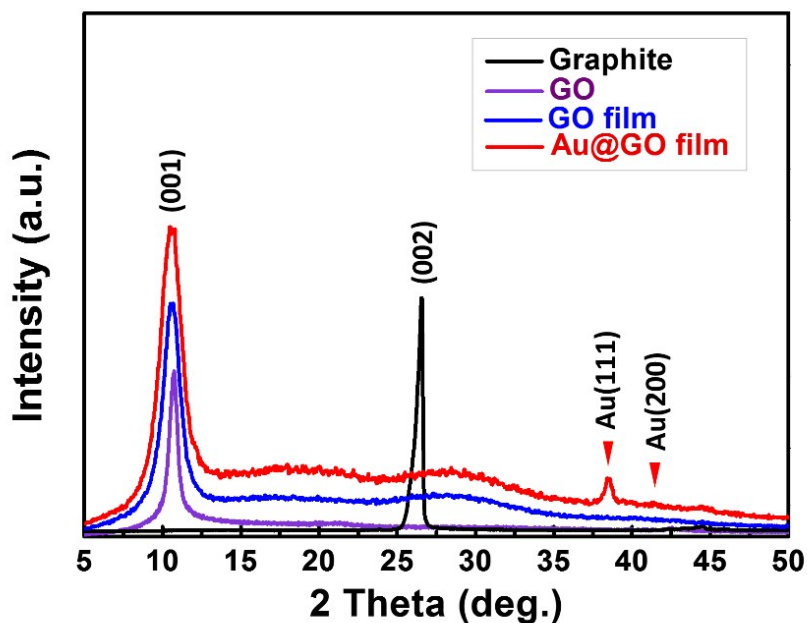


**Figure S5.** XRD patterns of the graphite, GO, GO film and Au@GO film. The crystalline XRD patterns of graphite, GO, GO film and Au@GO film (Figure 1h) demonstrated the formation of the samples. XRD spectra of Au@GO film includes three diffraction peaks, at scattering angle of  $10.5^\circ$  corresponding to a d-spacing 0.62 nm of crystal plane (0 0 1) of graphite oxide, and scattering angles of  $38.4^\circ$  and  $44.4^\circ$  matchup with crystal plane (1 1 1) and (2 0 0) of gold face-centered cubic crystallographic structure (JCPDS card No. 65-2870).<sup>9</sup> Above results of FESEM, EDS mapping, FTIR, Raman and XRD have demonstrated that we have obtained successfully the Au@GO film with thermal evaporation and evaporation coating method.

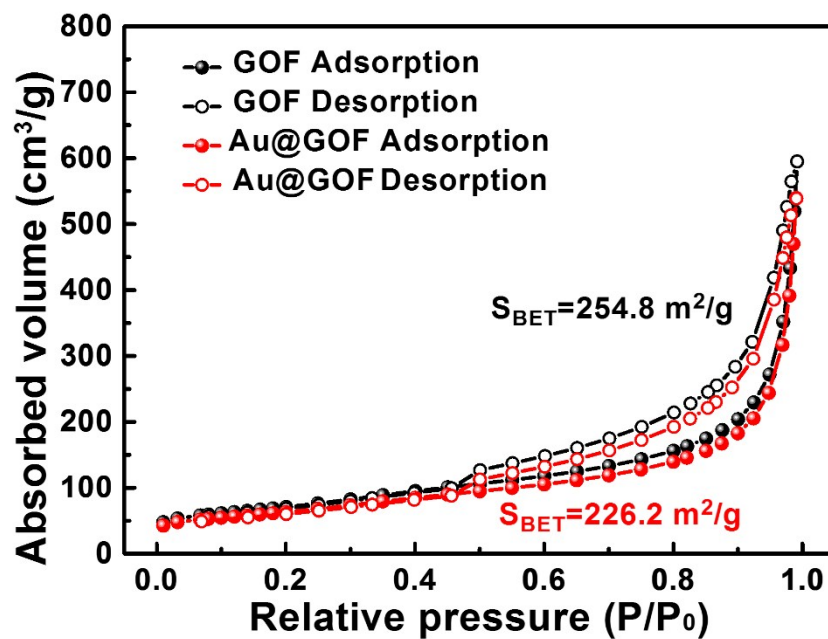


**Figure S6.** N<sub>2</sub> adsorption-desorption isotherms of the obtained GOF and Au@GOF. The Brunauer-Emmett-Teller (BET) analysis shows that the specific surface area of GOF and Au@GOF are up to 226.2 and 254.8 m<sup>2</sup>/g, respectively.

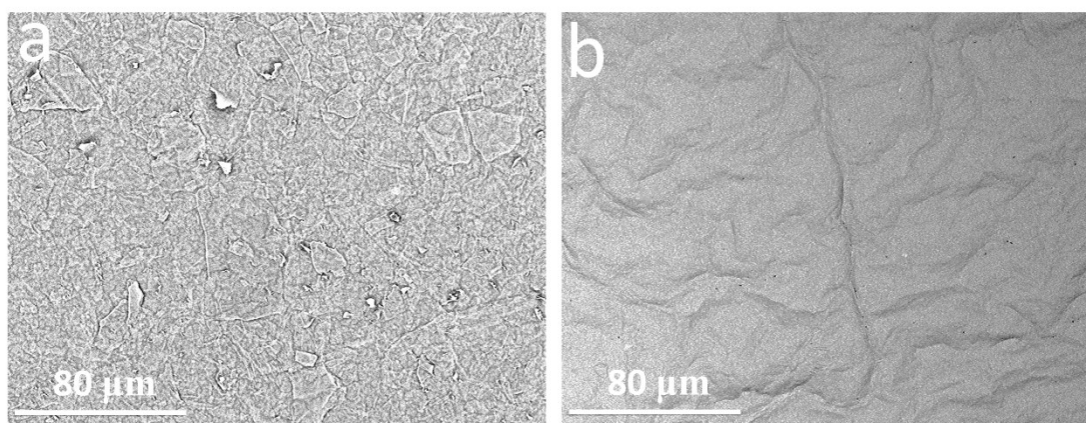


**Figure S7.** SEM images of the GO side (a) and the Au side (b) of Au@GO bilayer film.



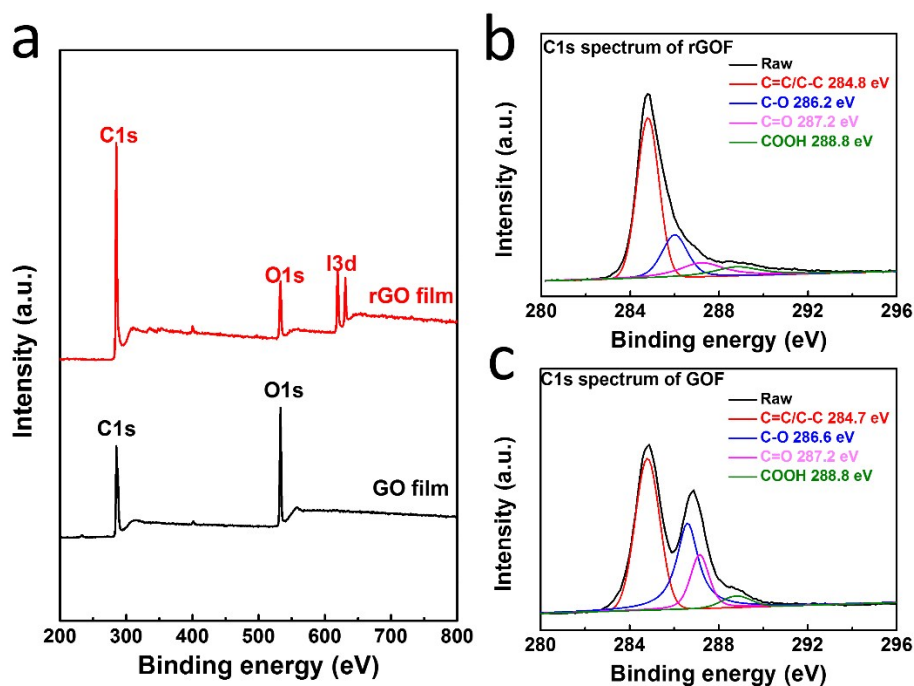


**Figure S8.** X-ray photoelectron spectra of rGOF, GOF. High resolution C1s spectrum of rGOF (b), GOF (c). The survey scan of GO side of Au@GOF showed the peaks of C1s and O1s in the ratio of 72.7: 27.3 (details are given in the Table 2, ESI †). The demonstrated C/O ratio of 2.7 corresponds to typical graphene oxide film.<sup>2, 10</sup> As shown in survey scan of rGO side of Au@rGOF, C, O and I peaks are clearly observed. The derived C/O ratio of 6.7 corresponds to typical chemically reduced graphene oxide.<sup>11</sup> Moreover, the high resolution spectrum shows the deconvoluted results of rGO side of Au@rGOF (Fig. b) and GO side of Au@GOF (Fig. c).

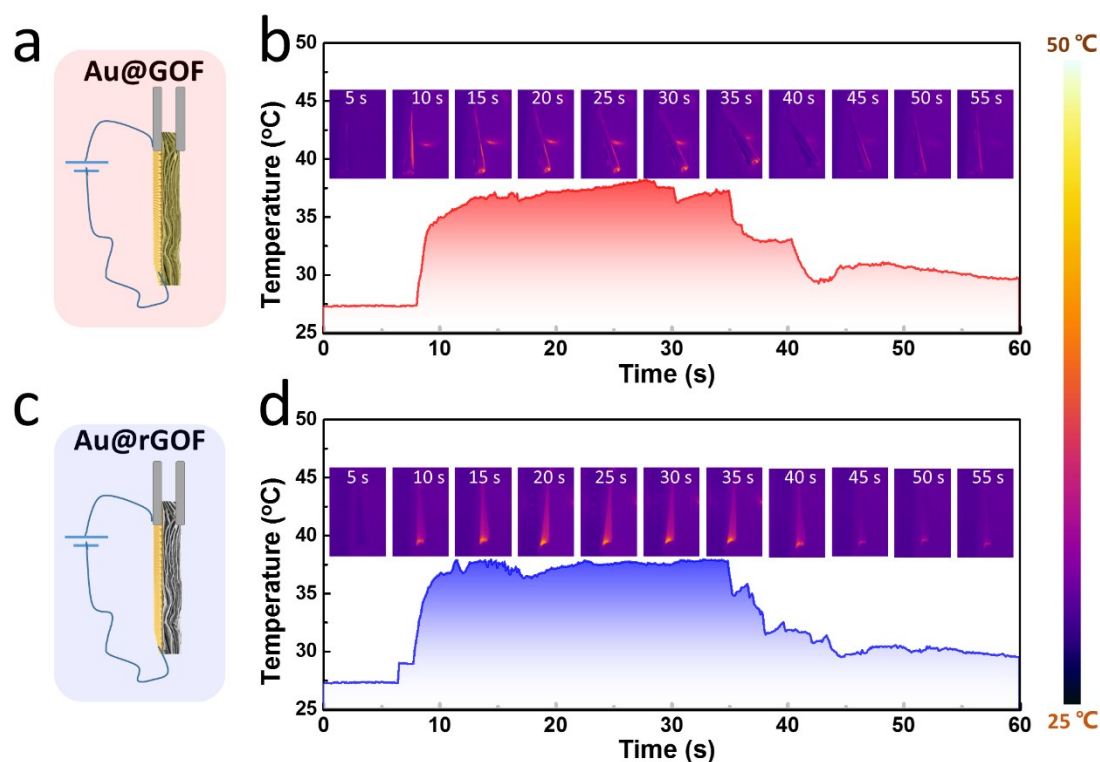


**Figure S9.** Electrical-driven behaviour of Au@GOF and Au@rGOF. Schematics of electrical-driven test circuit of Au@GOF (a) and Au@rGOF (c), respectively. Time-dependent surface temperature measurements of Au@GOF (b) and Au@rGOF (d) with 5 V direct voltage for about 30 s, respectively. Insets show corresponding infrared thermal images. The both temperature of Au@GOF and Au@rGOF increase up to about 37 °C from room temperature under 5 V direct voltage. The Au@GOF exhibits reversible electrical-driven actuation, but the Au@rGOF do not. The electrical actuation is clearly visible in Figure S9b insets and Video S1 (ESI†). The Au@rGOF do not exhibit such actuation behaviour in Figure S9d insets.

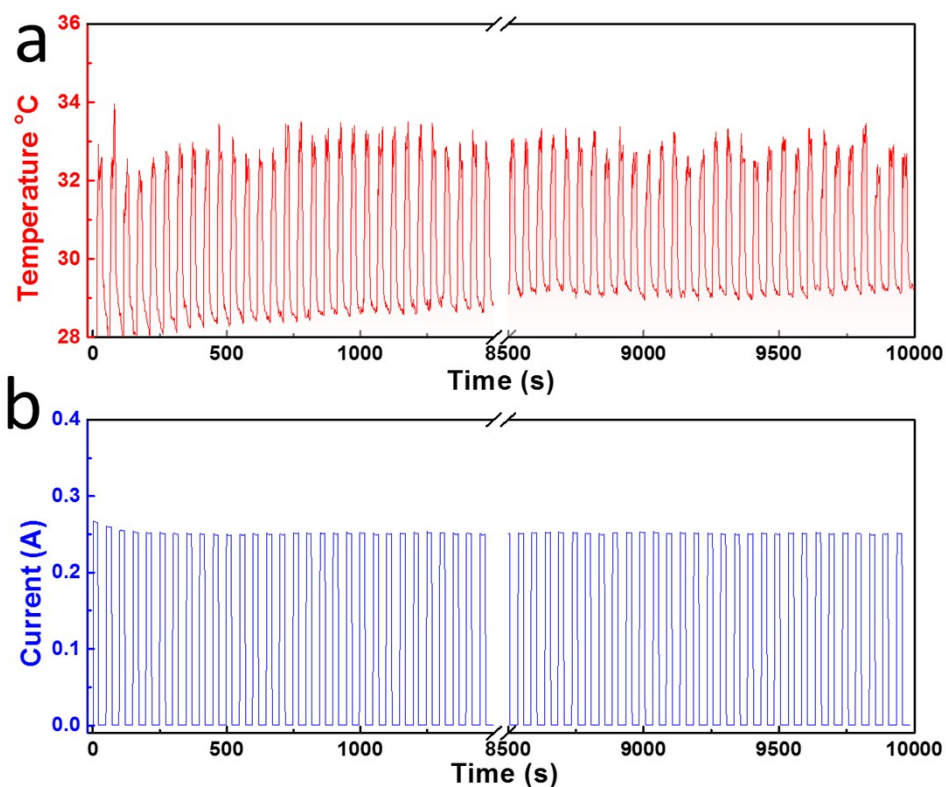


**Figure S10.** Cycle stability test of Au@GOF actuator. (a) Current-Time curve and corresponding (b) Temperature-Time curve of Au@GOF with the 4 V intervallic direct voltage for 200 cycles.

**Table 1.** Curve fitting results of XPS C1s spectrum.

	Peak	Binding energy (eV)	%
rGO side of Au@rGOF	C=C/C-C	284.8	60.2
	C-O	286.2	21.2
	C=O	287.2	14.6
	O=C-OH	288.8	4.0
GO side of Au@rGOF	C=C/C-C	284.7	46.5
	C-O	286.6	34.1
	C=O	287.2	15.1
	O=COH	288.8	4.3

**Table 2.** The content (At %) of C, O and I elementary of rGO side of Au@rGOF and GO side of Au@GOF.

	Spectrum	At. (%)
rGO side of Au@rGOF	C1s	86.6
	O1s	12.9
	I3d	1.5
GO side of Au@rGOF	C1s	72.7
	O1s	27.3

**Supplementary Video S1.** A real-time infrared thermal imaging of the electrical-driven bending behaviour of Au@GOF.

**Supplementary Video S2.** A real-time infrared thermal imaging of opening and closing state of the venus flytrap like Au@GOF electrical-driven actuator.

## Reference

1. W. S. Hummers and R. E. Offeman, *J. Am. Chem. Soc.*, 1958, 80, 1339-1339.
2. Q. W. Shi, C. Y. Hou, H. Z. Wang, Q. H. Zhang and Y. G. Li, *J. Mater. Chem. A*, 2015, 3, 9882-9889.
3. S. Fraser, X. Zheng, L. Qiu, D. Li and B. Jia, *Appl. Phys. Lett.*, 2015, 107, 031112.
4. A. R. Sadrolhosseini, A. S. M. Noor, N. Faraji, A. Kharazmi and M. A. Mahdi, *J. Nanomater.*, 2014, 2014, 1-8.
5. Z. Q. Niu, J. Chen, H. H. Hng, J. Ma and X. D. Chen, *Adv. Mater.*, 2012, 24, 4144-4150.
6. A. C. Ferrari and D. M. Basko, *Nat. Nano.*, 2013, 8, 235-246.
7. A. Gupta, G. Chen, P. Joshi, S. Tadigadapa and P. C. Eklund, *Nano Lett.*, 2006, 6, 2667-2673.
8. A. C. Ferrari, J. C. Meyer, V. Scardaci, C. Casiraghi, M. Lazzeri, F. Mauri, S. Piscanec, D. Jiang, K. S. Novoselov, S. Roth and A. K. Geim, *Phys. Rev. Lett.*, 2006, 97, 187401.
9. X. Huang, S. Li, S. Wu, Y. Huang, F. Boey, C. L. Gan and H. Zhang, *Adv. Mater.*, 2012, 24, 979-983.
10. B. T. McGrail, J. D. Mangadlao, B. J. Rodier, J. Swisher, R. Advincula and E. Pentzer, *Chem. Commun.*, 2016, 52, 288-291.
11. C. K. Chua and M. Pumera, *Chem. Commun.*, 2016, 52, 72-75.